Fluid Phase Equilibria 470 (2018) 51–59

Contents lists available at ScienceDirect

Fluid Phase Equilibria

journal homepage: www elsevier com/locate/fluid

Thermal behavior and heat capacities of pyrrolidinium-based ionic liquids by DSC

Elena Gómez [b], Noelia Calvar [b], Ángeles Domínguez [a], Eugénia A. Macedo [b,]

[a] Advanced Separation Processes Group, Department of Chemical Engineering, University of Vigo, Campus Lagoas-Marcosende, 36310 Vigo, Spain
[b] Associate Laboratory of Separation and Reaction Engineering – Laboratory of Catalysis and Materials LSRE-LCM), Department of Chemical Engineering, Faculty of Engineering, University of Porto, Rua Dr. Roberto Frias, s/n, Porto 4200-465, Portugal

R T I C L E I N F O

Article history:
Received 7 September 2017
Received in revised form
2 March 2018
Accepted 6 April 2018
Available online 7 April 2018

Keywords:
Pyrrolidinium ionic liquids
Heat capacity
Thermal behavior
DSC

B S T R C T

This work focuses on thermal study (melting, freezing, cold crystallization and glass transition temperatures have been determined) and on determination of heat capacities (in the temperature range from 293.15K to 333.15K) of several ionic liquids using differential scanning calorimetry. In order to study the effect of the anion and the alkyl-side chain of the cation of the ionic liquids on the thermal behavior and on the heat capacities values, the ionic liquids: 1-alkyl-1-methylpyrrolidinium bis(tri- uoromethylsulfonyl)imide [C_nMpyrNTf$_2$ (n 2,3,4)], 1-butyl-1-methylpyrrolidinium tri- uoromethanesulfonate (C_4MpyrTFO), and 1-butyl-1-methylpyrrolidinium dicyanamide (C_4MpyrDCA) were chosen. Besides, in order to analyze the in uence of the anion of the ionic liquid on the heat capacity, the results obtained in this study were compared with those obtained in our previous work (for the C_nMpyNTf$_2$ and C_nMimNTf$_2$ ionic liquids). Finally, the obtained results were compared with literature values.

© 2018 Elsevier B.V. All rights reserved.

1 Introduction

The interest in ionic liquids is mainly due to their special properties, among which can be highlighted: high thermal stability, high heat capacity and negligible vapor pressure for their potential applications in several fields; one of these applications is as replacements for current heat transfer uids (HTF) used in industry [1,2]. For the consideration of the ionic liquids as HTF, it is vital to determine their density, heat capacity, freezing and melting temperatures, heat of fusion, and thermal decomposition temperatures. With the differential scanning calorimetry (DSC) technique it is possible to obtain thermal properties, such as glass transition, melting, freezing, crystallization and cold crystallization temperatures. In addition, worth to mention that for most of ILs these thermal properties are unknown, in spite of being essential for the application of ILs to most of industrial processes, and particularly for their potential application as HTF and their heat storage performance.

This essay is a continuation of our previous work [3,4], in which a thermal study is carried out and the heat capacity of different ionic liquids is determined. In this work, the thermal behavior of several pyrrolidinium-based ionic liquids was analyzed and their heat capacities as function of temperature were determined using differential scanning calorimetry (DSC). To study the in uence of the alkyl chain length, the thermal behavior of 1-alkyl-1-methylpyrrolidinium bis(tri uoromethylsulfonyl)imide (C_nMpyrNTf$_2$) with n 2,3,4 has been analyzed, and the in uence of different anions was studied using the ionic liquids 1-butyl-1-methylpyrrolidinium tri- uoromethanesulfonate (C_4MpyrTFO), and 1-butyl-1-methylpyrrolidinium dicyanamide, (C_4MpyrDCA). Besides, in order to analyze the in uence of the anion of the ionic liquid on the heat capacity, the results obtained in this study were compared with those obtained in a previous publication (for the C_nMpyNTf$_2$ and C_nMimNTf$_2$ ionic liquids). Finally, both the obtained results of the thermal analysis [5–18] and the heat capacities were compared with literature values [16,19–21].

2 Experimental section

2.1. Chemicals

The ionic liquids studied in this work were acquired from IoLi-Tec, the mass fraction purity of all ionic liquids is higher than 0.99

Corresponding author.
E-mail address: eamacedo@fe.up.pt (E.A. Macedo).

https://doi.org/10.1016/j. uid.2018.04.003
0378-3812/© 2018 Elsevier B.V. All rights reserved.

except for C_4MpyrDCA that is higher than 0.98. All ionic liquids were further dried by stirring them at 343 K under a moderate vacuum of 0.2 Pa for at least 48 h prior to their use. Their purities and halide contents as analyzed by the suppliers together with the water content determined after the drying step with a Coulometric KF titrator, model C20 using Hydranal-Coulomat CG and Hydranal-Coulomat AG as cathodic and anodic titratans, are presented in Table 1. It is important to comment that in addition, the samples of ionic liquid were dried in situ in the DSC before each measurement. The structure of the ILs used in this work is shown in Fig. 1.

2.2. Apparatus and procedure

The Mettler-Toledo differential scanning calorimeter (DSC), model DSC822[e], was used for the studies of the thermal behavior of the pure ionic liquids and for the determination of their heat capacities. This DSC is joined to a liquid nitrogen cooling system in order to reach as low temperatures as 133.15 K. The calorimeter is also connected to an Olympus SC30 camera (CMOS color camera for light microscopy), which allows the visualization of the phase transitions, helping with their interpretation. The Mettler-Toledo STAR[e] software in its version 9.30 was used to evaluate the experimental data. As already explained in a previous work [3], the apparatus was calibrated for temperature and heat ow using pure zinc, indium, water and heptane and for tau lag by determining onset temperatures at different heating rates. The obtained reproducibility in the enthalpy of fusion and in temperature were ±2 and ±0.2 , respectively. In order to maintain a dry and inert atmosphere inside the furnace, dry nitrogen is constantly owing at 50 mL/min. The samples of pure ionic liquids were dried in situ in the furnace of the DSC by heating the sample at 403.15 K for 1 h. All the weighings carried out in this work were made using a Mettler-Toledo AX-205 Delta Range balance with an uncertainty in the measurement of $\pm 3 \times 10^{-4}$ g.

For the thermal analyses, 40 L aluminum pans hermetically sealed with a pinhole at the top were used for the samples and a similar empty pan also with a pinhole was used as the reference in the furnace. These pans (sample and reference) were chosen so that their weight was as close as possible to minimize errors in the measurements. The mass of the samples were relatively small, between 4 and 8 mg, to avoid homogenization errors and thermal lag. The temperatures used for the thermal analyzes range from 133.15 to 393.15 K at different cooling and heating rates. All the samples were subjected to a slow cooling and heating cycle at 2 K min^{-1} (slow method"), and depending on the obtained results, the run can be repeated at 10 K min^{-1} or, if there are freezing peaks, they are subjected to a quenching (cooling at 40 K min^{-1} and heating at 10 K min^{-1}) in order to prevent the IL from crystallizing

Table 1
Name, purity and halide contents supplied by the company and water content experimentally determined of the studied ionic liquids[a].

Ionic Liquid	Purity/ (mass fraction)	Halide content/(ppm)	Water content/(ppm)
C_2MpyrNTf$_2$[b]	≥0.99	100	150
C_3MpyrNTf$_2$[c]	≥0.99	100	100
C_4MpyrNTf$_2$[d]	≥0.99	100	70
C_4MpyrDCA[e]	≥0.98	200	300
C_4MpyrTFO[f]	≥0.99	100	160

[a] Standard uncertainty *u*(water content) ± 5 .
[b] 1-ethyl-1-methylpyrrolidinium bis(tri uoromethylsulfonyl) imide.
[c] 1-methyl-1-propylpyrrolidinium bis(tri uoromethylsulfonyl) imide.
[d] 1-butyl-1-methylpyrrolidinium bis(tri uoromethylsulfonyl) imide.
[e] 1-butyl-1-methylpyrrolidinium dicyanamide.
[f] 1-butyl-1-methylpyrrolidinium tri uoromethanesulfonate.

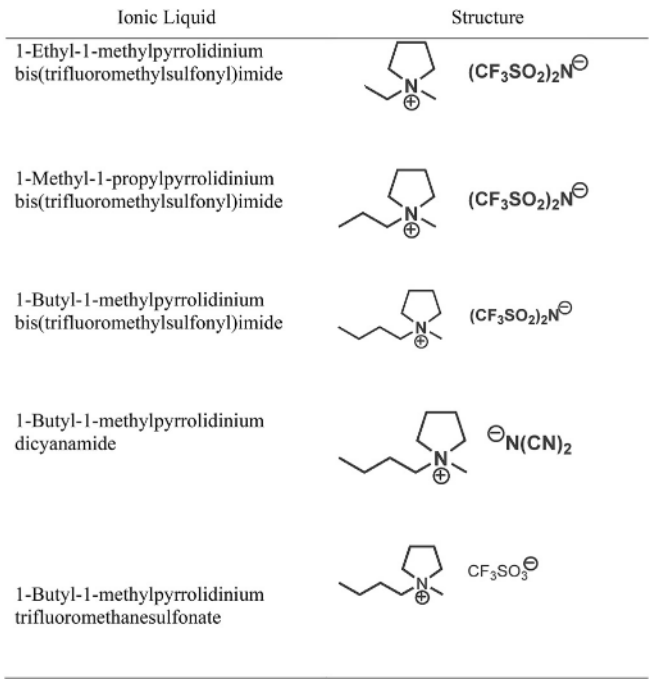

Fig 1 Structure of the ILs used in this work.

and thus be able to determine the glass transition. In the case that different crystals were observed, a more detailed study was carried out by cooling at 2 K min^{-1} and heating at different temperatures.

Regarding the understanding of the thermal scans, the melting temperature (Tm) was taken as the onset of an endothermic peak (downward de ection of the curve peak) on heating, the freezing temperature (Tf) as the onset of an exothermic peak (upward de ection of the curve peak) on cooling, the glass transition temperature (Tg) as the midpoint of a small heat capacity change on heating from the amorphous glass state to a liquid state, the cold crystallization temperature (Tcc) as the onset of an exothermic peak on heating from a subcooled liquid state to a crystalline solid state, the solid-solid transition (Tss) as the onset of an exothermic or endothermic peak on heating from a crystalline solid state.

For the determination of heat capacities a higher amount of sample is necessary since the size of the measurement signal is proportional to the sample amount, and thus 100 L aluminum pans hermetically sealed with a pinhole at the top were used. The sapphire method was used, consisting in an initial isothermal segment for 15 min followed by a dynamic period at 20 K min^{-1} and a final isothermal segment for 15 min. The runs for Cp measurements were repeated three times for each sample.

The calculated standard uncertainties are ±1K for the temperature in the thermal analysis and ±5 for the determination of the molar heat capacity. A more detailed explanation about the procedure can be found in literature [22], as well as the calculation of the standard uncertainties [3].

3 Results and discussion

3.1. Thermal analysis

Three different behaviors were found in the ionic liquids studied in this paper when the cooling and heating rate is 2 K min^{-1}, as in the case of the ionic liquids studied in previous papers [3,4]:

Table 2
Results of the thermal analysis for the studied ionic liquids[a].

	Rate/K min^{-1}	$Tf_{(L\ I)}$[b]/K	$Tf_{(I\ II)}$[c]/K	$Tf_{(II\ III)}$[d]/K	$Tf_{(III\ IV)}$[e]/K	Tg/K	Tcc/K	$Tss_{(IV\ III)}$[f]/K	$Tss_{(III\ II)}$[g]/K	$Tss_{(II\ I)}$[h]/K	$Tm_{(I)}$/K	$Tm_{(II)}$/K
$C_2MpyrNTf_2$	2	335	318	289	173			180	288	312	362	
	5	339	318	289	173			180	288	312	362	
	10	342	318	289	173			180	288	312	362	
	20	343	318	289	173			180	288	312	362	
	Q+10[i]	276						180	288	312	362	
$C_3MpyrNTf_2$	2	253									283	
	Q+10	[j]									284	
$C_4MpyrNTf_2$	2					183	208			244	253	
	5					185	213			244	252	
	10					187	217			244	254	
	1 without Tg[k]						208		240			262
	2 without Tg						211		235			263
	10 without Tg						220			244	252	
	20 without Tg						225			244	253	
$C_4MpyrTFO$	2	245								238	267	
	5	230							230	239	267	
	10	237								237	272	
	20	231								238	265	
$C_4MpyrDCA$	2					173						

[a] Standard uncertainty $u(T)$ ±1 K.
[b] Freezing temperature from liquid to crystal I.
[c] Freezing temperature from crystal I to crystal II.
[d] Freezing temperature from crystal II to crystal III.
[e] Freezing temperature from crystal III to crystal IV.
[f] Solid −solid transition temperature from crystal IV to crystal III.
[g] Solid −solid transition temperature from crystal III to crystal II.
[h] Solid −solid transition temperature from crystal II to crystal I.
[i] Cooling with quenching and heating at 10 K min^{-1}.
[j] Not readable with accuracy from thermal scan.
[k] Cooling the sample without reaching the glass transition temperature.

(i) the first type of behavior is formed by ionic liquids characterized by presenting only formation of amorphous glass;
(ii) the second type of behavior is characterized by presenting freezing, forming crystals on cooling. However, if they are subjected to quenching, a Tg is observed while the Tf disappears;
(iii) the third type of behavior appears in the ILs that do not show tendency to crystallize on cooling; however, on heating they show cold crystallization; The experimental values of the thermal transition temperatures of the studied ionic liquids are summarized in Table 2.

In Fig. 2 can be observed that if the ionic liquid $C_2MpyrNTf_2$ is subjected to the slow method", by cooling and heating at 2 K min^{-1}, the presence of four exothermic peaks on cooling and four endothermic peaks on heating (three small peaks at 180, 288 and 312 K and a larger peak at 362 K) is revealed.

To investigate in detail the endothermic peaks at 180, 288 and 312 K, the sample was subjected to different heating rates (5, 10 and

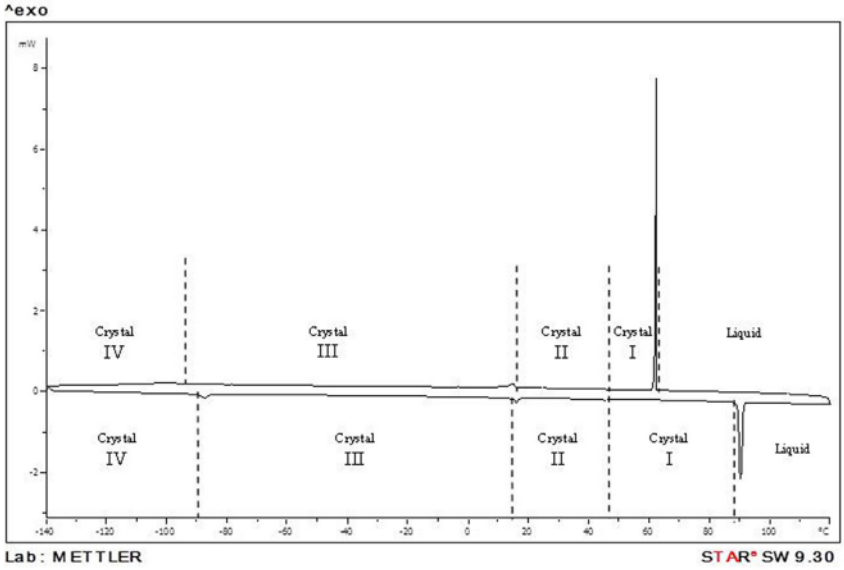

Fig 2 Thermal scan for $C_2MpyrNTf_2$ at a rate of 2 K min^{-1}.

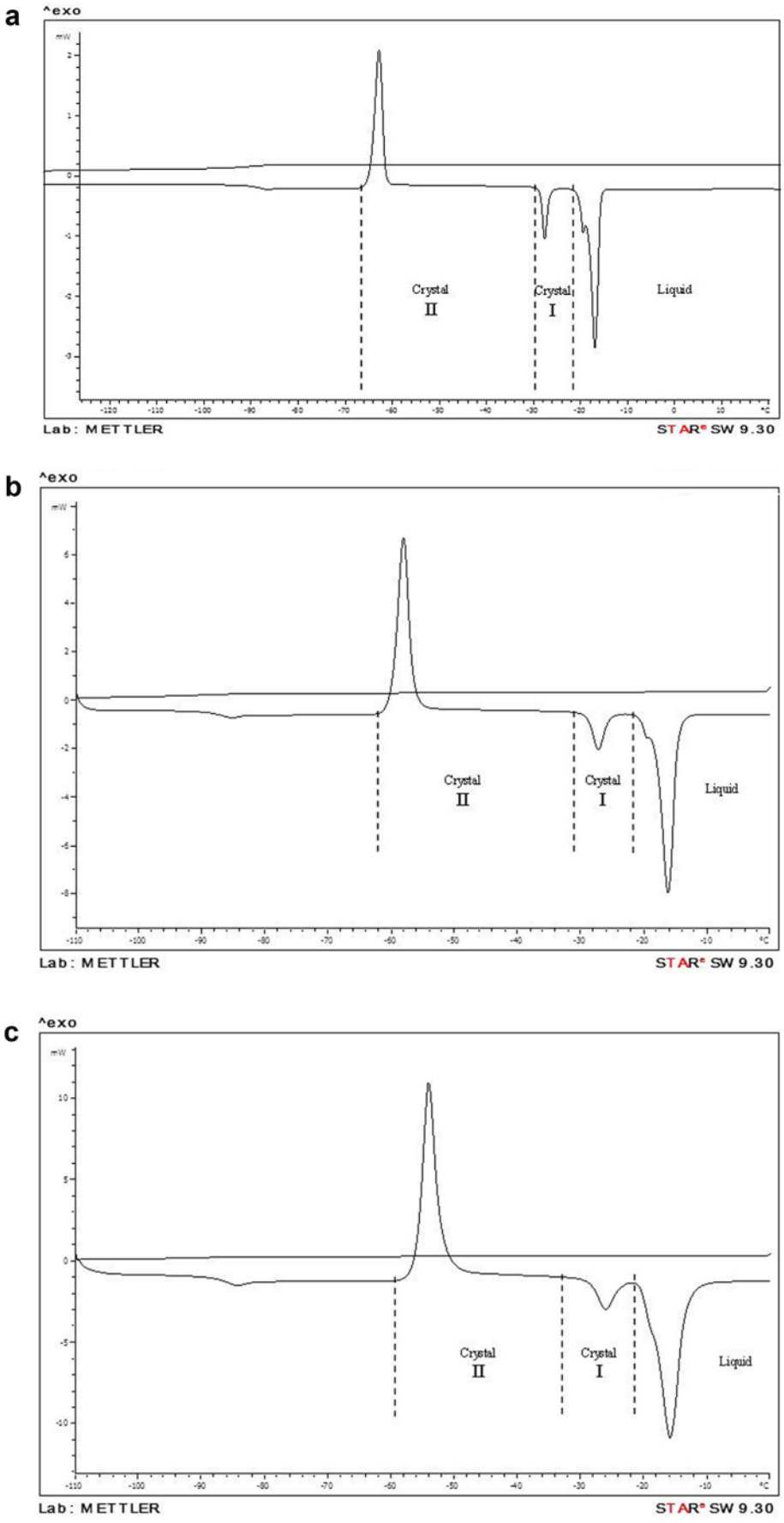

Fig 3 Thermal scan for $C_4MpyrNTf_2$ cooling the sample to 163K at 2 K min^{-1} and heating it up at a rate of a) 2 K min^{-1}, b) 5 K min^{-1} and c) 10 K min^{-1}.

20 K min^{-1}), after its cooling at 2 K min^{-1}. In these analyzes it was observed that the four transitions kept showing on cooling and on heating; therefore it can be assumed that they represent three solid-solid transitions of three different crystals, corroborating the idea that this ionic liquid forms different polymorphs when cooled. After stating the presence of polymorphs, a quenching method" was carried out, where a broad freezing peak on cooling and the three melting peaks were obtained, indicating that this ionic liquid is a strong crystal-former, as it is usual in ionic liquids with NTf_2^- as anion with short alkyl-side chain of the cation [3,4].

The ionic liquid $C_3MpyrNTf_2$ showed a freezing and a melting peak (at 253 K and 283 K, respectively) when subjected to the slow method". When a quenching is applied to the sample, it also presented the same peaks (the freezing peak moved to lower temperatures). In video V1 available in Supplementary data the instantaneous freezing suffered by this ionic liquid can be observed. Both this ionic liquid and the previous one ($C_3MpyrNTf_2$) belong to the second type of behavior previously explained.

The ionic liquid $C_4MpyrNTf_2$ has the behavior explained in the third type, i.e., it does not form crystals on cooling while on heating it presents a glass transition followed by a cold crystallization and three endothermic peaks, as shown in Fig. 3. To study these endothermic peaks, the sample was subjected to different heating rates and it was recorded to visually assess the transitions. By cooling the sample at 2 K min^{-1} and heating it up at 5 or 10 K min^{-1} the glass transition and the cold crystallization appeared at higher temperatures as the heating rate increases, which is a behavior already observed for other ILs [3,4], but the three endothermic peaks appeared approximately at the same temperatures than when the sample was heated at 2 K min^{-1}, although it should be noted that the second and third peak are joined, increasingly indistinguishable as the heating rate increases, as it can be observed in Fig. 3a)–c). With the help of the video, where no visible changes were observed at 244 K (a melting transition would be visible), it can be stated that the transition is a solid-solid transition where all or part of the crystals formed in the cold crystallization change their conformation. According to the movements seen in the video, it can be said that at 252 K a conformational change immediately followed by a melting transition (occasionally they can occur at the same time) is the reason for these two overlapped peaks.

Knowing that it is likely that this IL forms several polymorphs (due to the nature of the anion and the cation), several runs were carried out by cooling the sample without reaching the glass transition temperature to check if different crystals are formed. Therefore, the samples were cooled to 193 K at 2 K min^{-1} and heated at 1, 2, 10 and 20 K min^{-1}. From the curves obtained for these experiments, it can be observed that when the sample is heated at 1 and 2 K min^{-1} the Tcc appears at 208 and 211 K respectively, followed by one or two exothermic peaks (Tss) at 240 K for the heating rate of 1 K min^{-1} and 235 and 245 K for 2 K min^{-1}, and the appearance of one small and one large endothermic peaks at approximately 262 and 265 K. It should be remarked that the exothermic peaks following the Tcc are broad irregular peaks. In video V2 available in Supplementary data, the change in the crystals occurred at 240 K can be clearly observed. On the other hand, when the samples are heated at 10 and 20 K min^{-1} the shape of the curves are similar to those obtained when the sample is cooled to 133 K, i.e., beyond the glass transition temperature. Examples of these behaviors are shown in Fig. 4.

In summary, when depending on the conditions the glass formed in the cold crystallization suffers an endothermic solid-solid transition at 244 K, the ionic liquid presents another solid-solid transition immediately followed by its melting at approximately 254 K, that is, in the cold crystallization transition a type II crystal is formed, which changes to a type I crystal in the endothermic solid-solid transition at 244 K which melts at 254 K (Fig. 4a). On the other hand, when the Tcc glass suffers an exothermic solid-solid transition at approximately 240 K the other solid-solid transition joined to the melting occurs at approximately

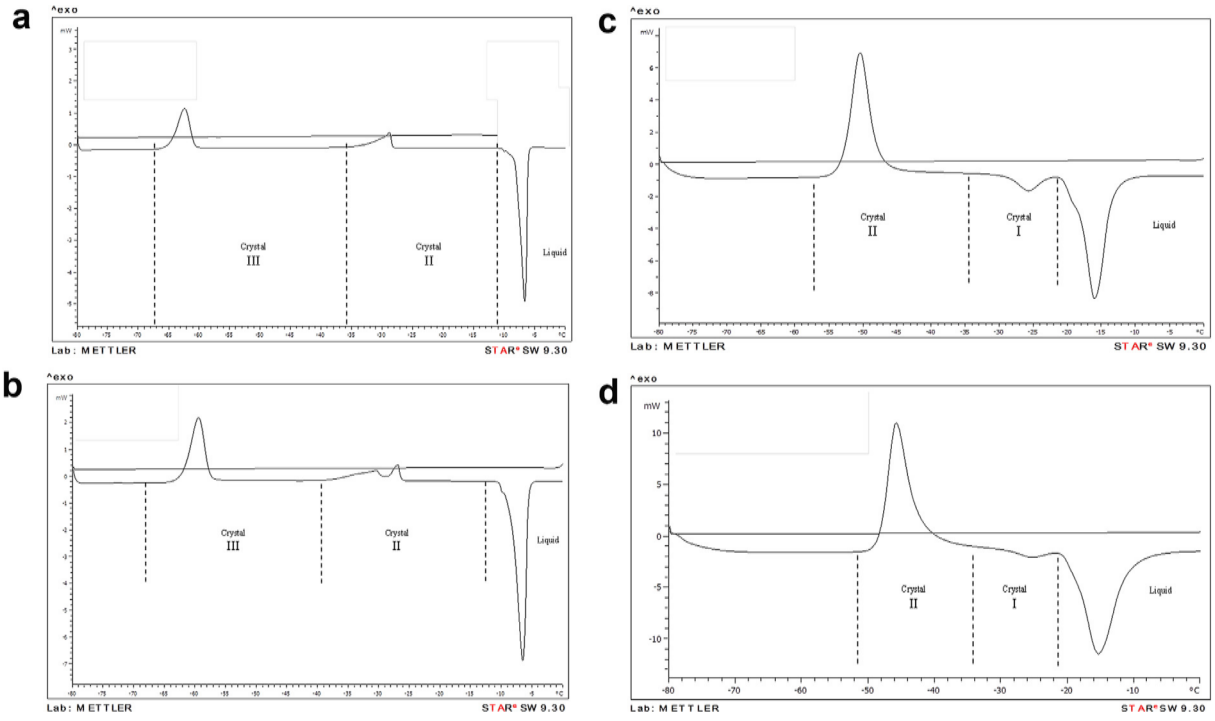

Fig 4 Thermal scan for $C_4MpyrNTf_2$ cooling the sample to 193K at 2 K min^{-1} and heating it up at a rate of a) 1 K min^{-1}, b) 2 K min^{-1}, c) 10 K min^{-1} and d) 20 K min^{-1}.

265 K, that is, the cold crystallization transition gives rise to a type III crystal which changes to a type II crystal in the exothermic Tss which melts at 265 K (Fig. 4b).

The ionic liquid C_4MpyrTFO presents the same behavior than C_2MimNTf$_2$ and C_3MpyrNTf$_2$, i.e., it belongs to the second type of behavior where the ionic liquid forms crystals on cooling and melts on heating (Fig. S1 a) available in Supplementary data). In the case of this ionic liquid, unlike the transition shown by C_3MpyrNTf$_2$, the freezing was not instantaneous, as shown by the broad and irregular peaks (up to three) represented in the DSC curve and video V3 presented in Supplementary data where movements along a temperature range can be observed, suggesting the possibility of the existence of polymorphs. On the process of heating, this ionic liquid suffers a small endothermic transition at 238 K followed by a broad and irregular melting transition. Using the video V4 (Supplementary data), it can be said that the endothermic transition is a solid-solid transition where some of the crystal or crystals formed on cooling change their conformation. Regarding the following broad endothermic curve, movements of changing crystals can be observed immediately mixed with a melting process; therefore, in that broad peak a solid-solid transition is occurring while some of the crystals melt to finally lead to the melting of the whole sample.

Given the possibility of the formation of different crystals in this IL, additional experiments were carried out with the same cooling rate (2 K min^{-1}) and different heating rates (5, 10 and 20 K min^{-1}). In these curves the same behavior was found, with the peak comprising the solid-solid and the melting transitions becoming wider as the heating rate increases. However, when the heating rate was 5 K min^{-1} another small endothermic curve at 230 K appeared, suggesting the presence of a solid-solid transition. Given the appearance of freezing transitions on cooling and two solid-solid transitions on heating, at least three crystals have been formed during the experiments.

Finally, this IL was subjected to a quenching method and it showed to be a strong crystal former, since it still suffered freezing on cooling despite the relatively high cooling rate.

The ionic liquid C_4MpyrDCA showed the first type of behavior (Fig. S1b) available in Supplementary data), presenting only a glass transition at approximately −100 °C.

In Table 3 the experimental results from the thermal analyses are compared with literature values [5–18]. As it can be observed, the results obtained in this work are in agreement with those in literature when the experimental conditions are similar. Besides this, with the new experiments carried out, these ionic liquids are

Table 3
Literature comparison for the thermal analysis of the studied ionic liquids.

		Rate	$Tf_{(L\ I)}$	$Tf_{(I\ II)}$	$Tf_{(II\ III)}$	$Tf_{(III\ IV)}$	Tg	Tcc	$Tss_{(IV\ III)}$	$Tss_{(III\ II)}$	$Tss_{(II\ I)}$	$Tm_{(I)}$	$Tm_{(II)}$
C_2MpyrNTf$_2$	This work	2	335	318	289	173			180	288	312	362	
	This work	5	339	318	289	173			180	288	312	362	
	This work	10	342	318	289	173			180	288	312	362	
	This work	20	343	318	289	173			180	288	312	362	
	[5]	10					171			173	287	359	
	[6]	na.							187	290	318	363	
	[7]	na							188	290	318	364	
	[8]	na					183		183	291	318	361	
	[9]	20					168	172	186	287	293	363	
C_3MpyrNTf$_2$	This work	2	253									283	
	This work	Q+10										284	
	[10]	10	~258[a]				183					282	
	[11]	2	259									283	
	[11]	5	261									283	
	[11]	10	262									284	
	[12]	2/10										283	
	[5]	10					183	206		228	255	285	
	[13]	20/10										285	
	[14]	10										284.6	
	[8]	na					183	198[a]		228[a]	255[a]	285	
	[15]	10										283	
C_4MpyrNTf$_2$	This work	2					183	208			244	253	
	This work	5					185	213			244	252	
	This work	10					187	217			244	254	
	This work	1 without Tg						208		240			262
	This work	2 without Tg						211		235			263
	This work	10 without Tg						220			244	252	
	This work	20 without Tg						225			244	253	
	[16]	na					181				240		
	[10]	10					188				244	256	
	[11]	Q 1st cycle					186	217			239	252	
	[11]	Q 2nd cycle					186	217			$^{(II-I+II)}$240	252	262
	[11]	10					181	204		226			262
	[12]	Q					188	220			$^{(II-I+II)}$243	255	
	[5]	na					186	218[a]			249	255	
	[13]	20/10											267
	[14]	10											266
	[6]	na											266
	[17]	10					190					258	
	[8]	na					186	218[a]			249	255	
	[18]	na											266
	[15]	10					186	220				255	

na not available.
[a] Read on graphic presented in the original reference.

Table 4
Experimental molar heat capacities, c_p, for the studied ionic liquids (phase liq).[a]

T/K	c_p/J K^{-1} mol^{-1}			T/K	cp/J K^{-1} mol^{-1}
	$C_4MpyrNTf_2$	$C_4MpyrTFO$	$C_4MpyrDCA$		$C_3MpyrNTf_2$
293.15	566	432	407	323.15	567
294.15	568	434	408	324.15	569
295.15	569	435	410	325.15	571
296.15	570	437	411	326.15	573
297.15	571	438	412	327.15	575
298.15	572	439	413	328.15	576
299.15	573	441	414	329.15	578
300.15	574	442	416	330.15	579
301.15	574	443	417	331.15	581
302.15	575	444	418	332.15	582
303.15	576	445	419	333.15	584
304.15	577	446	420	334.15	585
305.15	578	448	421	335.15	586
306.15	578	449	422	336.15	588
307.15	579	450	422	337.15	589
308.15	580	451	423	338.15	590
309.15	581	452	424	339.15	591
310.15	581	453	425	340.15	593
311.15	582	454	426	341.15	594
312.15	583	455	427	342.15	595
313.15	583	456	428	343.15	597
314.15	584	457	429	344.15	598
315.15	585	458	429	345.15	599
316.15	585	459	430	346.15	600
317.15	586	460	431	347.15	601
318.15	587	460	432	348.15	601
319.15	588	461	433	349.15	602
320.15	588	462	434	350.15	604
321.15	589	463	434	351.15	604
322.15	590	464	435	352.15	605
323.15	590	465	436	353.15	606
324.15	591	466	437		
325.15	592	467	438		
326.15	593	468	439		
327.15	593	469	440		
328.15	594	470	441		
329.15	595	471	442		
330.15	596	472	442		
331.15	596	473	443		
332.15	597	474	444		
333.15	598	475	445		

[a] Uncertainty is $u(c_p)$ ±5 .

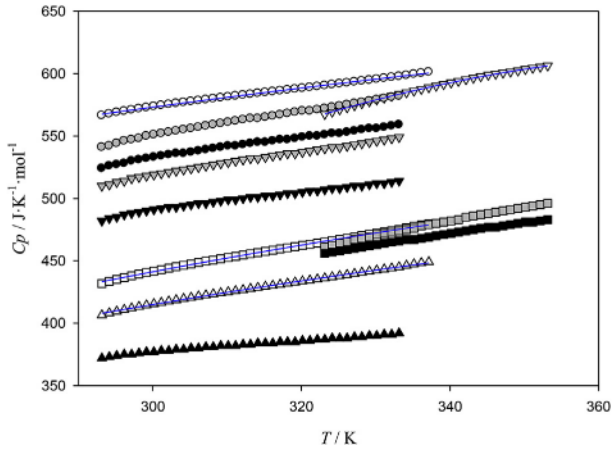

Fig 5 Experimental molar heat capacities, c_p, determined in this work and in previous works as a function of temperature. Symbols: , $C_3MpyrNTf_2$ (this work); ○, $C_4MpyrNTf_2$ (this work); △, $C_4MpyrDCA$ (this work); , $C_4MpyrTFO$ (this work); ▼, $C_3MpyNTf_2$ (reference [4]); ●, $C_4MpyNTf_2$ (reference [4]); ■, $C_4MpyTFO$ (reference [4]); ▼, $C_3MimNTf_2$ (reference [3]), ●, $C_4MimNTf_2$ (reference [3]); ■, $C_4MimTFO$ (reference [3]); ▲ ,$C_4MimDCA$ (reference [3]); (−), solid blue lines represent the fitting using the quadratic equation. (For interpretation of the references to color in this figure legend, the reader is referred to the Web version of this article.)

Table 5
Fitting parameters for the fitting (C_p y_0+aT +bT^2) of the experimental heat capacities.

IL	y_0	a	b	R^2
$C_3MpyrNTf_2$	−1540.5	11.319	−0.0148	0.9998
$C_4MpyrNTf_2$	166.15	1.9095	−0.0018	0.9985
$C_4MpyrTFO$	−188.08	3.0622	−0.0320	0.9987
$C_4MpyrDCA$	−130.18	2.6340	−0.0027	0.9984

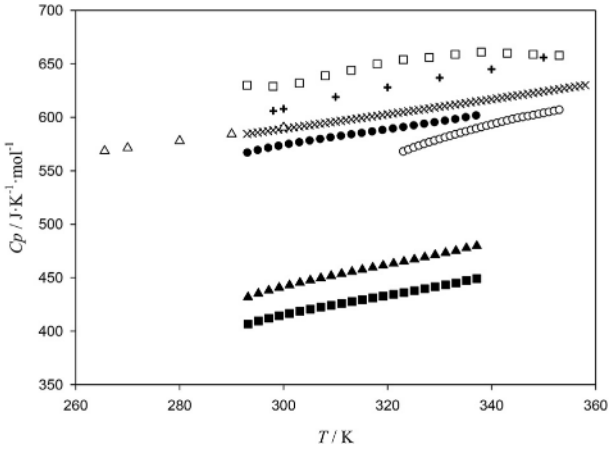

Fig 6 Experimental molar heat capacities determined in this work and literature values as a function of temperature. Symbols: ○, $C_3MpyrNTf_2$ (this work); ●, $C_4MpyrNTf_2$ (this work); ■, $C_4MpyrDCA$ (this work); ▲, $C_4MpyrTFO$ (this work); △, $C_4MpyrNTf_2$ (reference [16]); , $C_4MpyrNTf_2$ (reference [19]); X, $C_4MpyrNTf_2$ (reference [20]); +, $C_4MpyrNTf_2$ (reference [21]).

better characterized. The comparison of results is sometimes difficult due to the different procedures and to the fact that sometimes the experiment setups are not well defined.

3.2. Heat capacities

Heat capacities scans were completed from (258.15−348.15) K. However, only data from (293.15−333.15) K are presented since at the temperature range limits the samples are not fully thermally conditioned [22].

The experimental heat capacities for the all ionic liquids studied in this work in the temperature range T (293.15−333.15) K are summarized in Table 4 and these experimental data are also plotted in Fig. 5. In this figure the heat capacities of ionic liquids with pyridinium and imidazolium cation determined in our previous work [3,4] are also represented, in order to evaluate the in uence of cation of the ionic liquid in the value of the heat capacity.

If the heat capacity of the $C_nMpyrNTf_2$ ILs are compared it can be observed that longer alkyl chains on the cation, increase the C_p; this behavior agrees with that reported in literature [19,23] and with the results of our previous work (as also shown in Fig. 5) for $C_nMpyNTf_2$ and $C_nMimNTf_2$ ILs.

Regarding the heat capacities of ILs with the same cation and different anions, in this work it can be observed that an increase in the size of the anion means an increase of the C_p values. For the ionic liquids with 1-buthyl-3methylpyrrolidinium cation the C_p values at 298.15 K decrease in the order $NTf_2^- > TFO^- > DCA^-$, the same result was found for the ionic liquids with the pyridinium cation (Fig. 5) and this behavior agrees with that found in literature [19,23].

Finally, in Fig. 5 if we compare the ionic liquids with the same anion and the same alkyl chain but different anion type, in all cases,

the pyrrolidinium-based ionic liquid present higher heat capacities than their analogous pyridinium-based ionic liquid and these present higher heat capacities than imidazolium-based ionic liquids.

The dependence of the heat capacities with temperature is usually fitted to a polynomial. In this work, a quadratic polynomial equation (C_p y_0+aT + bT^2) was used to fit the obtained heat capacities, and the fitting parameters for the studied ILs are presented in Table 5 together with the squared correlation factor, R^2. As it can be inferred from this table, with R^2 values higher than 0.99, the heat capacities follow a good linear trend with temperature. This fitting can be also observed in Fig. 5.

In Fig. 6, a comparison between experimental and literature values [16,19–21] of heat capacities as function of the temperature is presented for C_4MpyrNTf$_2$ ionic liquid. The largest deviations (>9) have been found related to the data published by Hardacre et al. [19]. The deviation between the experimental values and those recommended by Paulechka in his review [20] for this ionic liquid is 2 . In general, the deviation values are close of the uncertainty in the measurement of the heat capacities. For the ionic liquid C_4MpyrDCA there is published in the bibliography [23,24] the value of C_p 502 J K^{-1} mol^{-1} at T 298.15K, the difference with the value published in this work is about 21 , although this difference it may be due to the different methods chosen for the experimental determination of C_p, while that in this work the C_p has been determined from 258.15 to 348.15 K, in the previous works [23,24] the method used was from 293 to 333 K. For the rest of ionic liquids presented in this work no literature data were found.

4 Conclusions

The determination of the thermal analysis and the heat capacities of the several pyrrolidinium-based ionic liquids C_nMpyrNTf$_2$ (n 2,3,4), C_4MpyrTFO and C_4MpyrDCA has been carried out with a Mettler-Toledo differential scanning calorimeter (DSC), model DSC822^e combined with the Mettler-Toledo STAR^e software, version 9.30 and an Olympus SC30 camera (CMOS color camera for light microscopy).

The thermal behavior of the ionic liquid was determined following a specific protocol, finding three types of thermal behavior: the first type of behavior is formed by ionic liquids characterized by only present a glass transition, the second type is characterized by presenting freezing, forming crystals on cooling and finally, the third type appears in the ILs that do not show tendency to crystallize on cooling; however, on heating they show cold crystallization.

The experimental results were compared with those found in literature, and the comparison showed a satisfactory agreement.

The heat capacities increased linearly with temperature for all studied ionic liquids and it was concluded that the heat capacity values of the pyrrolidinium ionic liquids with the NTf$_2^-$ anion increase as the alkyl-side chain of the cation increases. Regarding the in uence of the cation on the heat capacities of ILs, in this work it can be observed that an increase in the size of the anion means an increase of the C_p values. Finally, the pyrrolidinium-based ionic liquid present higher heat capacities than their analogous pyridinium-based ionic liquid and these present higher heat capacities than imidazolium-based ionic liquids.

Acknowledgments

This work is a result of project AIProcMat@N2020 - Advanced Industrial Processes and Materials for a Sustainable Northern Region of Portugal 2020", with the reference NORTE-01-0145-FEDER-000006, supported by Norte Portugal Regional Operational Programme (NORTE 2020), under the Portugal 2020 Partnership Agreement, through the European Regional Development Fund (ERDF) and of Project POCI-01-0145-FEDER-006984 – Associate Laboratory LSRE-LCM funded by ERDF through COMPETE2020 - Programa Operacional Competitividade e Internacionalização (POCI) – and by national funds through FCT - Fundacao para a Ciencia e a Tecnologia. Elena Gómez thanks funding support from Project: AIProcMat@N2020-01-0145-FEDER-000006 and Noelia Calvar is grateful for the scholarship from Fundaçao para a Ciencia e a Tecnologia (FCT, Portugal) (ref.SFRH/BDP/37775/2007). Authors also thank to the Ministerio de Economía, Industria y Competitividad (Spain) for financial support through the project CTQ2016-77422-C2-1-R (AEI/FEDER, UE).

Appendix A Supplementary data

Supplementary data related to this article can be found at https://doi.org/10.1016/j. uid.2018.04.003.

References

[1] J.M. Franca, C.A.N. De Castro, M.M. Lopes, V.M.B. Nunes, In uence of thermophysical properties of ionic liquids in chemical process design, J. Chem. Eng. Data 54 (2009) 2569–2575.
[2] C.A.N. De Castro, E. Langa, A.L. Morais, M.L.M. Lopes, M.J. Lourenço, F.J. Santos, M.C.S. Santos, J.N.C. Lopes, H.I. Veiga, M. Macatrao, J.M.S.S. Esperança, C.S. Marques, L.P. Rebelo, C.A. Afonso, Studies on the density, heat capacity, surfase tension and infinite dilution diffusion with ionic liquids C4minNTf2, C4mimDCA, C2mim EtSO4 and Aliquat DCA, Fluid Phase Eq. 294 (2010) 157–159.
[3] E. Gómez, N. Calvar, A. Domínguez, E.A. Macedo, Thermal analysis and heat capacities of 1-alkyl-3-methylimidazolium ionic liquids with NTF$_2$, TFO and DCA anions, Ind. Eng. Chem. Res. 52 (2013) 2103–2110.
[4] N. Calvar, E. Gómez, E.A. Macedo, A. Domínguez, Thermal analysis and heat capacities of pyridinium and imidazolium ionic liquids, Thermochim. Acta 565 (2013) 178–182.
[5] D.R. MacFarlane, P. Meakin, J. Sun, N. Amini, M. Forsyth, Pyrrolidinium imides: a new family of molten salts and conductive plastic crystal phases, J. Phys. Chem. B 103 (1999) 4164–4170.
[6] T. Fox, Joshua E.F. Weaver, Wesley A. Henderson, Tuning binary ionic liquid mixtures: linking alkyl chain length to phase behavior and ionic conductivity eric, J. Phys. Chem. C 116 (2012) 5270–5274.
[7] A. Wesley, Henderson, G. Victor, Young Jr., P. Stefano, C. Paul, Trulove, C. Hugh, De Long, Plastic phase transitions in N-Ethyl-N-methylpyrrolidinium bis(tri uoromethanesulfonyl)imide, Chem. Mater. 18 (2006) 934–938.
[8] D.R. MacFarlane, P Meakin1, N Amini1, M Forsyth. Structural studies of ambient temperature plastic crystal ion conductors, J. Phys. Condens. Matter 13 (2001) 8257–8267.
[9] A.J. Hill, J. Huang, J. Efthimiadis, P. Meakin, M. Forsyth, D.R. MacFarlane, Microstructural and molecular level characterisation of plastic crystal phases of pyrrolidinium tri uoromethanesulfonyl salts, Solid State Ionics 154–155 (2002) 119–124.
[10] Gary Annat, Maria Forsyth, Douglas R. MacFarlane, Ionic liquid mixtures: variations in physical properties and their origins in molecular structure, J. Phys. Chem. B 116 (2012) 8251–8258.
[11] Claudia Simona Stefan, Daniel lemordant philippe biensan, Cle'mence siret, Be'nédicte claude-montigny thermal stability and crystallization of N-alkyl-N-alkyl0-pyrrolidinium imides, J. Therm. Anal. Calorim. 102 (2010) 685–693.
[12] Miriam Kunze, Sangsik Jeong, Elie Paillard, Martin Winter, Stefano Passerini, Melting behavior of pyrrolidinium-based ionic liquids and their binary mixtures, J. Phys. Chem. C 114 (2010) 12364–12369.
[13] Miriam Kunze, Maria Montanino, Giovanni B. Appetecchi, Sangsik Jeong, Monika Schönhoff, Martin Winter, Stefano Passerini, Melting behavior and ionic conductivity in hydrophobic ionic liquids, J. Phys. Chem. A 114 (2010) 1776–1782.
[14] Giovanni B. Appetecchia, Maria Montaninoa, Maria Carewskaa, Margherita Morenoa, Fabrizio Alessandrinia, Stefano Passerini, Chemical–physical properties of bis(per uoroalkylsulfonyl)imide-based ionic liquids, Electrochim. Acta 56 (2011) 1300–1307.
[15] Hui Jin, Bernie O'Hare, Jing Dong, Sergei Arzhantsev, Gary A. Baker, James F. Wishart, Alan J. Benesi, Mark Maroncelli, Physical properties of ionic liquids consisting of the 1-butyl-3-methylimidazolium cation with various anions and the bis(tri uoromethylsulfonyl)imide anion with various cations, J. Phys. Chem. B 112 (2008) 81–92.
[16] Yoshitaka Shimizu, Yoko Ohte, Yasuhisa Yamamura, Seiji Tsuzuki, Kazuya Saito, Comparative study of imidazolium- and pyrrolidinium-based ionic liquids: thermodynamic properties, J. Phys. Chem. B 116 (2012) 5406–5413.
[17] Hiroyuki Tokuda, Kunikazu Ishii, Md Abu Bin Hasan Susan, Seiji Tsuzuki, Kikuko Hayamizu, Masayoshi Watanabe, Physicochemical properties and

structures of room-temperature ionic liquids. Variation of cationic structures, J. Phys. Chem. B 110 (2006) 2833–2839.
[18] M. Montaninoa, M. Morenoa, F. Alessandrinia, G.B. Appetecchia, S. Passerinib, Q. Zhouc, W.A. Henderson Physical and electrochemical properties of binary ionic liquid mixtures: (1 –x)PYR14TFSI–(x) PYR14IM14, Electrochim. Acta 60 (2012) 163–169.
[19] R.GeC. Hardacre, J. Jacquemin, P. Nancarrow, D.W. Rooney, Heat capacities of ionic liquids as a function of temperature at 0.1 MPa. Measurement and prediction, J. Chem. Eng. Data 53 (2008) 2148–2153.
[20] U. Yauheni, Paulechka heat capacity of room-temperature ionic liquids: a critical review, J. Phys. Chem. Ref. Data 39 (2010).
[21] C. Jagadeeswara Rao, R. Venkata Krishnan, K.A. Venkatesan, K. Nagarajan, T.G. Srinivasan, Thermochemical properties of some bis(tri uoromethyl-sulfonyl)imide based room temperature ionic liquids, J. Therm. Anal. Calorim. 97 (2009) 937–943.
[22] E. Gómez, N. Calvar, A. Domínguez, Thermal behaviour of Pure Ionic Liquids (Chapter 8 of the Book: Ionic Liquids-Current State of Art), INTECH, 2015, pp. 199–229.
[23] E.J. Gónzalez, A. Domínguez, E.A. Macedo, Physical and excess properties of eight binary mixtures containing water and ionic liquids, J. Chem. Eng. Data 57 (2012) 2165–2176.
[24] E.J. Gónzalez, B. Gónzalez, E.A. Macedo, Thermophysical properties of the pure ionic liquids 1-butyl-1-methylpyrrolidinium dicyanamide and its binary mixtures with alcohols, J. Chem. Eng. Data 58 (2013) 1440–1448.